Davies et al. New Zealand Journal of Forestry Science (2016) 46:19
DOI 10.1186/s40490-016-0075-x

New Zealand Journal of Forestry Science

SHORT REPORT Open Access

Elastic constants of green *Pinus radiata* wood

Nicholas T. Davies*, Clemens M. Altaner and Luis A. Apiolaza

Abstract

Background: Mathematical modelling is often used to investigate phenomena difficult or impossible to measure experimentally.

Findings: This paper presents the constants needed to mathematically model green *Pinus radiata* D.Don core- and outerwood. The constants include all three elastic and shear moduli along with the six Poisson ratios needed for describing orthotropic materials in the elastic domain. Further proportional limit surfaces are presented.

Conclusions: The constants provided allow for an increase in realism of mathematical models examining the mechanical performance of standing trees.

Keywords: Corewood, Elastic modulus, Never-dried, Poisson ratio, Shear modulus, Strength

Findings

Introduction

Mathematical modelling is increasingly being used to investigate tree biomechanics (Ciftci et al. 2013; Coutand et al. 2011; Fourcaud et al. 2002; Fourcaud and Lac 2002; Guillon et al. 2012; Moore and Maguire 2008; Ormarsson et al. 2010; Sellier et al. 2006; Wagner et al. 2012). Such models need to be parameterised with material constants expressing the elastic behaviour as well as failure characteristics. Wood is often described as an orthotropic material, implying independent material properties for the radial, tangential and longitudinal direction (Bodig and Jayne 1982). Nine independent material constants are required to describe the elastic behaviour of orthotropic materials, including elastic moduli, shear moduli and Poisson ratios.

The failure characteristics of wood are complex. A simple way to express the failure characteristics is proportional limits. These are defined as the point at which stress and strain stop being linearly related. Proportional limit surfaces can be used to describe the proportional limit when a material is deformed in multiple directions at once. This is different to ultimate tensile failure which is the point when catastrophic failure occurs within a sample resulting in two separate pieces. Wood is also a hygroscopic material, and its mechanical behaviour is influenced by changes in moisture content (Skaar 1988). As wood is usually used in a dry state, most published material constants for wood are for the dry state (e.g. Ross 2010) which are a poor representation when modelling live trees.

A further complication is that wood as a biomaterial varies greatly in its properties even within a tree. Radial changes in wood properties within trees are well documented (Lachenbruch et al. 2011). Also, most research on these radial patterns within stems focused on longitudinal material properties, neglecting material properties in transverse direction. These radial gradients are particularly important when considering younger trees, for example from commercial fast-growing, short-rotation plantations (Zobel and Sprague 1998).

Full sets of material constants for green wood are hard to find. A number of full or near full sets of elastic constants for wood above fibre saturation, along with other texts of interest, are provided in Additional file 1. To the best of our knowledge, no full sets of material constants have been published for green corewood.

The constants used to parameterise mathematical tree models are generally estimated from generic relationships to known properties, typically in longitudinal direction and below fibre saturation point due to a lack of empirical values. The purpose of this paper is to provide the material constants necessary for describing green core- and outerwood as an orthotropic material. Tree stems can

* Correspondence: ntd14@uclive.ac.nz
New Zealand School of Forestry, College of Engineering, University of Canterbury, Private Bag, 4800 Christchurch, New Zealand

Springer Open

© 2016 The Author(s). **Open Access** This article is distributed under the terms of the Creative Commons Attribution 4.0 International License (http://creativecommons.org/licenses/by/4.0/), which permits unrestricted use, distribution, and reproduction in any medium, provided you give appropriate credit to the original author(s) and the source, provide a link to the Creative Commons license, and indicate if changes were made.

be modelled more realistically with the provided data. The study used *Pinus radiata* D.Don selected from plantations in Canterbury, New Zealand.

Materials and method

Green *P. radiata* boards cut from trees approximately 28 years old were sourced from a sawmill in Canterbury, New Zealand. Four boards (50 × 100 × 2400 mm), two outerwood and two corewood, were chosen from approximately 30 boards to represent high and low green density and dynamic modulus. Corewood (found adjacent to the pith) was defined as wood with widely spaced rings and high ring curvature, and outerwood (found adjacent to the bark) as the opposite (Burdon et al. 2004). No distinction could be made regarding the tree(s) the boards came from nor heights of the samples in the trees.

The samples were stored in sealed bags with excess water at 5 °C for a maximum period of 2 weeks. Subsequently, six defect-free, straight-grained test specimens of the required shape and orientation were machined from each of the four boards, totalling in 216 (6 replicates × 4 boards × 3 orientations × 3 tests) test specimens. All testing was conducted at room temperature and humidity over the 2-week period. Prior to mechanical testing, each specimen was weighed and its volume measured by water displacement. Acoustic velocity was measured using TREETAP, a prototype non-destructive direct transmission time-of-flight acoustic tool developed at the University of Canterbury.

The specimens were placed into a universal testing machine (UTM) (Instron 5566). Displacement was tracked on the two faces perpendicular to the axis of loading with two digital cameras fitted with 60-mm macro lenses taking images every 3 s.

The UTM fitted with a load cell (0.1-N accuracy) was run at a constant velocity of 1.5 mm min^{-1} for 300 s. For compression testing, the samples with dimensions of 30 × 15 × 15 mm were used, with the 30-mm direction under load. Tension testing used bone-shaped samples with dimensions 50 × 25 × 6.5 mm with the breakage plane having an area of 6.5 × 6.5 mm. With the exception of the longitudinal direction, where a straight stick test of dimensions 100 × 6.5 × 6.5 mm was used, with the 100-mm direction under load. For the shear plane, L-shaped samples with a shear plane of 15 × 15 mm were used. Once the specimens had been mechanically tested, they were oven-dried at 104 °C, weighed and volume-measured using the displacement method. The micro-fibril angle (MFA) and standard deviation of the micro-fibrils for one specimen of each sample and test (i.e. 12 in total) were obtained using X-ray diffraction (Cave and Robinson 1998a, 1998b).

Stress-strain curves were created from photo collections and the time/load UTM data via Digital Image Correlation and Tracking Matlab scripts (Eberl et al. 2006). One-dimensional average strains were taken in both the vertical and horizontal directions. Elastic moduli E, Poisson ratios ν and limits of proportionality were derived from the linear portion of the stress-strain curve. For each test of each specimen, a visual inspection of the stress-strain curve was undertaken and the initial reorientation of the sample discarded. The linear portion of the stress-strain curve was then identified by overlaying a linear model to the data. The elastic region was defined as the region with the least deviation between the data and the model. Orthotropic materials have a symmetry giving rise to Eq. 1 (Salençon 2001).

$$\frac{\nu_{tr}}{E_t}=\frac{\nu_{rt}}{E_r},\quad \frac{\nu_{lr}}{E_l}=\frac{\nu_{rl}}{E_r},\quad \frac{\nu_{tl}}{E_t}=\frac{\nu_{lt}}{E_l} \tag{1}$$

Where the elastic modulus (E) is in the direction of the subscript, r (radial), t (tangential) or l (longitudinal) and ν (Poisson ratio) with the first subscript being the direction of load, and the second subscript being the perpendicular direction of measured dimension change. These equalities did not hold in these experiments, due to samples deviating from orthotropic behaviour or errors inherent in the method of measurement. The discrepancy has been reported previously by Walker (1961). In order to ensure these equalities hold, optimisation was used to find the values which deviate least from all of the experimental values while still satisfying the equality constraints (Eq. 1). The deviation (the difference between the mean experimental value and the updated theoretical value which satisfies the constraints) was normalised against the 95 % confidence intervals of the mean values in order to give every variable an even weighting. The optimisation uses the constraints in Eq. 1 and the objective function in Eq. 2.

$$min\sum\frac{|\delta_i-\gamma_i|}{\theta_i}\qquad i=E_r,\ E_t,\ E_l,\ \nu_{rt},\ \nu_{tr},\ \nu_{tl},\ \nu_{lt},\ \nu_{lr},\ \nu_{rl} \tag{2}$$

where δ_i is the experimental value of i, γ_i is the corrected value of i, and θ_i is the 95 % confidence interval of δ_i. The 99.9 % confidence interval was used for the stiff high-density tension sample.

The Tsai and Wu (1971) failure criterion provides a general theory of strength for anisotropic materials. Wood has been reported to behave differently under compression and tension (Bodig and Jayne 1982; Ozyhar et al. 2013), so separation of the two load types is needed for the strength criteria. This theory has been applied to wood and wood products previously (Mackenzie-Helnwein et al. 2005; Mackenzie-Helnwein et al. 2005).

In the simplified case used here, the off-diagonal terms (governing interaction between material directions) are ignored giving the version of the Tsai and Wu (1971) failure criterion presented in Eqs. 3–10.

$$\boldsymbol{\sigma}^T\boldsymbol{q}+\boldsymbol{\sigma}^T\boldsymbol{P}\boldsymbol{\sigma}-1=0 \tag{3}$$

$$\boldsymbol{\sigma} = \begin{bmatrix} \sigma_r \\ \sigma_t \\ \sigma_l \\ \sigma_{tl} \\ \sigma_{lr} \\ \sigma_{rt} \end{bmatrix} \tag{4}$$

$$\boldsymbol{q} = \begin{bmatrix} F_{rr} \\ F_{tt} \\ F_{ll} \\ 0 \\ 0 \\ 0 \end{bmatrix} \tag{5}$$

$$P = \begin{bmatrix} F_{rrrr} & 0 & 0 & 0 & 0 & 0 \\ 0 & F_{tttt} & 0 & 0 & 0 & 0 \\ 0 & 0 & F_{llll} & 0 & 0 & 0 \\ 0 & 0 & 0 & F_{tltl} & 0 & 0 \\ 0 & 0 & 0 & 0 & F_{lrlr} & 0 \\ 0 & 0 & 0 & 0 & 0 & F_{rtrt} \end{bmatrix} \tag{6}$$

$$F_{ii} = \frac{1}{f_{it}} - \frac{1}{f_{ic}} \qquad i = r, t, l \tag{7}$$

$$F_{ij} = \frac{1}{f_{ijt}} - \frac{1}{f_{ijc}} \qquad i, j = r, t, l \quad (i \neq j) \tag{8}$$

$$F_{iiii} = \frac{1}{f_{it} f_{ic}} \qquad i = r, t, l \tag{9}$$

$$F_{ijij} = \frac{1}{f_{ij}^{\,2}} \qquad i, j = r, t, l \quad (i \neq j) \tag{10}$$

Proportional limit surfaces were calculated using Eqs. 3–10 in two dimensions.

Ultimate failure is difficult to define in the compression case, so this criterion is reported only for the tensile tests. In the tensile direction, ultimate failure results in a sudden drop in stress when the sample breaks.

Table 1 Descriptive wood properties of the samples tested

Property	Stiff outerwood	Non-stiff outerwood	Stiff corewood	Non-stiff corewood
Green density (kg m^{-3})	1143 (3)	1099 (9)	933 (21)	818 (22)
Dry density (kg m^{-3})	531 (5)	458 (9)	438 (8)	393 (5)
Acoustic velocity (m s^{-1})	4651 (8)	4221 (26)	4191 (34)	3413 (14)
Number of rings	>20	>20	<10	<10
MFA (degrees)	7 (1)	8 (1)	9 (2)	21 (1)
Standard deviation of MFA (degrees)	9 (1)	12 (1)	11 (1)	12 (0)

Mean values of tested wood properties for the sample types. Standard errors are in brackets. The reported standard deviation for the micro-fibril angle (MFA) is the value of the standard deviation parameter fitted to the model used to describe the micro-fibril spread around the mean (Cave and Robinson 1998a; 1998b)

Table 2 Elastic moduli and Poisson ratios for green core- and outerwood *Pinus radiata*

Direction	Stiff outerwood	Non-stiff outerwood	Stiff corewood	Non-stiff corewood
E_r (GPa)	0.49	0.3	0.26	0.31
E_t (GPa)	0.25	0.19	0.24	0.17
E_l (GPa)	4.36	2.81	3.5	2.38
TL (GPa)	0.11	0.21	0.11	0.13
LR (GPa)	0.06	0.03	0.04	0.03
RT (GPa)	0.05	0.02	0.02	0.04
v_{rt}	0.64	0.54	0.60	0.77
v_{rl}	0.03	0.05	0.03	0.06
v_{tr}	0.33	0.33	0.55	0.42
v_{tl}	0.03	0.01	0.03	0.04
v_{lr}	0.29	0.47	0.36	0.44
v_{lt}	0.60	0.16	0.37	0.50

Elastic moduli (*E*) and Poisson ratios (*υ*) optimised for the orthotropic assumption. Subscripts define the load direction (*r* = radial; *t* = tangential; *l* = longitudinal), and the terms *TL*, *LR* and *RT* define the shear planes

Results and discussion

A number of descriptive properties of the samples are presented in Table 1. The outerwood boards were of higher dry density and lower MFA (and in turn, faster acoustic velocity), resulting in a higher longitudinal

Table 3 Mean proportional limits for green core- and outerwood of *Pinus radiata*

Direction	Stiff outerwood (MPa)	Non-stiff outerwood (MPa)	Stiff corewood (MPa)	Non-stiff corewood (MPa)
rt_t	0.8 (0.2)	1.3 (0.5)	1.2 (0.3)	0.9 (0.1)
rt_c	−3.2 (0.1)	−2.5 (0.2)	−2.1 (0.1)	−3.2 (0.3)
rl_t	1.0 (0.1)	0.8 (0.2)	1.7 (0.4)	0.5 (0.1)
rl_c	−3.3 (0.2)	−2.6 (0.1)	−2.3 (0.1)	−3.3 (0.2)
tr_t	0.8 (0.2)	0.7 (0.2)	0.9 (0.1)	0.6 (0.1)
tr_c	−0.27 (0.1)	−2.4 (0.3)	−1.8 (0.2)	−2.0 (0.2)
tl_t	1.0 (0.3)	0.5 (0.1)	0.8 (0.2)	0.8 (0.2)
tl_c	−2.6 (0.2)	−2.8 (0.2)	−2.0 (0.1)	−2.3 (0.3)
lr_t	46.0 (7.5)	26.0 (1.3)	7.6 (1.8)	21.8 (4.1)
lr_c	−17.4 (1.0)	−6.6 (2.9)	−14.0 (1.1)	−17.6 (1.9)
lt_t	35.3 (3.8)	27.0 (4.5)	9.6 (2.4)	20.6 (2.4)
lt_c	−15.5 (1.5)	−8.5 (3.5)	−13.6 (1.6)	−21.4 (2.8)
TL	2.2 (0.4)	4.5 (0.3)	2.7 (0.2)	3.2 (0.3)
LR	1.8 (0.1)	0.9 (0.2)	1.6 (0.3)	1.3 (0.1)
RT	1.1 (0.2)	0.6 (0.2)	0.7 (0.1)	0.9 (0.1)

Mean proportional limit values: the first letter is the direction of force (with respect to the grain (*r* = radial; *t* = tangential; *l* = longitudinal)); the first and second letters describe the face which was recorded (e.g. *rt* = radial tangential); and the third letter distinguishes between a tension force, *t*, and a compressive force, *c*. For example, rt_t a tension force (the subscript *t*) is applied in the radial direction (the first letter), and the camera is imaging the radial tangential plane (the first two letters). The terms TL, LR and RT define the shear planes. Standard errors are in brackets

dynamic modulus as has been widely reported (Lachenbruch et al. 2011). Extreme values for corewood differed more than for outerwood, with the stiff corewood sample being of similar properties as the non-stiff outerwood sample (Additional file 2).

Variation in the measurements represents not only experimental error but also the underlying inhomogeneity of wood. The confounding effect between board and wood type should be noted as only a single board was chosen to represent each wood type. It is not possible to separate these two effects without a larger study. Additional file 2 provides the mean and standard error of elastic (in both tension and compression tests) and shear moduli. Additional file 3 provides the mean and standard error of the Poisson ratios, from both tensile and compression testing.

The elastic moduli and Poisson ratios for extreme cases of never-dried outerwood and corewood of *P. radiata* are presented in Table 2. The values were obtained through optimisation and averaging. The Poisson ratios were calculated from the compressive tests; the elastic moduli were taken from data collected from tangential-radial faces where possible or averaged from all four faces for the longitudinal direction. Tension and compression values were averaged and optimised. Elastic moduli calculated from tensile and compressive testing have been shown to differ by 21.4 % previously (Walker 1961) which is of a similar order of magnitude as is reported here. The constants presented here, although similar, tend to be lower than in other reported studies (for a comparison, see Additional file 1). This result was expected given the species and moisture content. The stiffer corewood sample showed properties similar to or exceeding that of the non-stiff outerwood sample. Poisson ratios showed little dependence on wood type or longitudinal stiffness.

The limits of proportionality calculated with no interaction terms for extremes of never-dried outerwood and corewood of *P. radiata* are shown in Table 3. The behaviour of the two corewood samples was of interest.

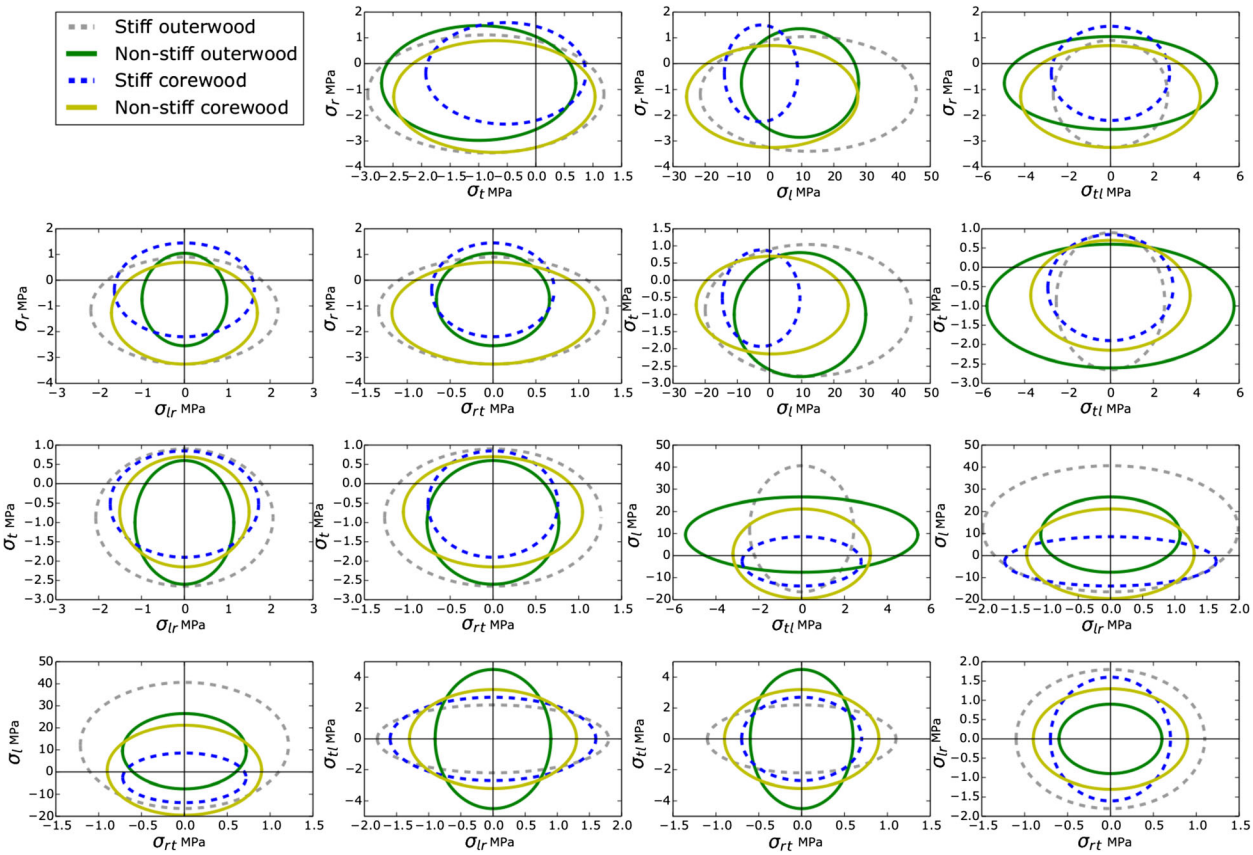

Fig. 1 Elastic proportional limit surfaces for all failure planes. *Ellipses* show the transition from the elastic to the non-elastic region (proportional limit surfaces) calculated using the Tsai and Wu (1971) failure criterion with no interaction terms for all failure planes of green *Pinus radiata* core- and outerwood. Axes show stress (σ) in the direction of the subscript, where two subscripts represent a shear stress is in the plane described by the subscripts. All directions not on the displayed axes are set to zero

The outerwood samples were stronger in longitudinal tension than in compression while the corewood samples were more centred on the origin. This difference can also be seen in the proportional limit surfaces (Fig. 1) which show the propensity for never-dried outerwood to be strongest under axial tension. An interesting phenomenon occurred with decreasing density. The samples became more centred or even favoured compression in the longitudinal direction.

The mean values and standard errors of ultimate tensile strength are shown in Table 4. The tangential strength values overlap for all wood types. Stiff corewood has a lower longitudinal strength than non-stiff corewood, while the opposite holds true for outerwood. As discussed previously, a confounding effect of board and wood type could not be excluded. Also note that two values are reported for the strength in each direction because two faces were tracked during the experiment. These can be averaged to give a more robust value.

The results showed that it can be important to consider the differences between corewood and outerwood when modelling the mechanical behaviour of trees. The presented data will allow researchers to build more realistic biomechanical models of trees.

Conclusion

Different material properties should be considered when mathematically treating tree stems as engineered structures because of the mechanical differences between core- and outerwood. Wood properties should be derived from samples in the green state that most closely represents the living tissue. Here, the nine elastic constants needed to represent an orthotropic material are presented for green core- and outer-wood *P. radiata*. Green core- and outerwood reach limits of proportionality at different strains in different directions. Proportionality limit surfaces are also presented.

Table 4 Mean ultimate tensile strength of green core- and outerwood of *Pinus radiata*

Direction	Stiff outerwood (MPa)	Non-stiff outerwood (MPa)	Stiff corewood (MPa)	Non-stiff corewood (GPa)
rt	3.1 (0.3)	3.1 (0.3)	2.9 (0.2)	2.2 (0.2)
rl	3.1 (0.3)	3.0 (0.3)	2.8 (0.3)	2.2 (0.2)
tr	2.1 (0.4)	1.6 (0.3)	1.9 (0.1)	2.1 (0.2)
tl	2.1 (0.5)	1.4 (0.3)	1.9 (0.1)	2.1 (0.2)
lr	64 (6)	45 (5)	21 (2)	33 (3)
lt	65 (6)	44 (6)	20 (2)	33 (3)

The first letter is the direction of force(r = radial; t = tangential; l = longitudinal), the first and second letters describe the face on which the strain was recorded (rt = radial tangential etc). Standard errors of the means are in brackets

Additional files

Additional file 1: Literature values of elastic constants for wood above the fibre saturation point. (docx 357 kb)

Additional file 2: Mean elastic moduli obtained for extremes of green core- and outerwood of *Pinus radiata*. (docx 221 kb)

Additional file 3: Mean Poisson ratios for green core- and outerwood *Pinus radiata*. (docx 215 kb)

Abbreviation

MFA: Micro-fibril angle; UTM: Universal testing machine

Acknowledgements

The authors wish to thank New Zealand Foundation for Research, Science and Technology Compromised Wood (P2080) Programme for financial support.

Authors' contributions

ND designed and carried out the experimental work, data analysis and paper preparation. CA contributed to experimental design and paper preparation. LA contributed to data analysis. All authors read and approved the final manuscript.

Competing interests

The authors declare that they have no competing interests.

Received: 21 January 2016 Accepted: 27 September 2016
Published online: 16 October 2016

References

Bodig, J., & Jayne, B. A. (1982). *Mechanics of wood and wood composites*. New York: Van Nostrand Reinhold.

Burdon, R. D., Kibblewhite, R. P., Walker, J. C. F., Megraw, R. A., Evans, R., & Cown, D. J. (2004). Juvenile versus mature wood: a new concept, orthogonal to corewood versus outerwood, with special reference to *Pinus radiata* and *P. taeda*. *Forest Science, 50*(4), 399–415.

Cave, I., & Robinson, W. T. (1998a, 1998). *Interpretation of (002) diffraction arcs by means of a minimalist model.* Paper presented at the IAWA/IUFRO International Workshop on the Significance of Microfibril Angle to Wood Quality, Westport, New Zealand.

Cave, I., & Robinson, W. T. (1998b, 1998). *Measuring microfibril angle distribution in the cell wall by means of x-ray diffraction.* Paper presented at the IAWA/IUFRO International Workshop on the Significance of Microfibril Angle to Wood Quality, Westport, New Zealand.

Ciftci, C., Brena, S. F., Kane, B., & Arwade, S. R. (2013). The effect of crown architecture on dynamic amplification factor of an open-grown sugar maple (Acer saccharum L.). *Trees-Structure and Function, 27*, 1175–1189. doi:10.1007/s00468-013-0867-z.

Coutand, C., Mathias, J.-D., Jeronimidis, G., & Destrebecq, J.-F. (2011). TWIG: a model to simulate the gravitropic response of a tree axis in the frame of elasticity and viscoelasticity, at intra-annual time scale. *Journal of Theoretical Biology, 273*, 115–129. doi:10.1016/j.jtbi.2010.12.027.

Eberl, C., Thompson, R., Gianola, D., & Bundschuh, S. (2006). *Digital Image Correlation and Tracking with Matlab.*

Fourcaud, T., & Lac, P. (2002). Numerical modelling of shape regulation and growth stresses in trees. *Trees-Structure and Function, 17*, 23–30. doi:10.1007/s00468-002-0202-6.

Fourcaud, T., Blaise, F., Lac, P., Castéra, P., & Reffye, P. d. (2002). Numerical modelling of shape regulation and growth stresses in trees. *Trees-Structure and Function, 17*, 31–39. doi:10.1007/s00468-002-0203-5.

Guillon, T., Dumont, Y., & Fourcaud, T. (2012). Numerical methods for the biomechanics of growing trees. *Computers & Mathematics with Applications, 64*, 289–309. doi:10.1016/j.camwa.2012.02.040.

Lachenbruch, B., Moore, J. R., & Evans, R. (2011). Radial variation in wood structure and function in woody plants, and hypotheses for its occurrence. In C. F. Meinzer, B. Lachenbruch, & E. T. Dawson (Eds.), *Size- and age-related changes in tree structure and function* (pp. 121–164). Dordrecht: Springer Netherlands.

Mackenzie-Helnwein, P., Eberhardsteiner, J., & Mang, H. A. (2005). Rate-independent mechanical behavior of biaxially stressed wood: experimental

observations and constitutive modeling as an orthotropic two-surface elasto-plastic material. *Holzforschung, 59*, 311–321.
Mackenzie-Helnwein, P., Müllner, H. W., Eberhardsteiner, J., & Mang, H. A. (2005). Analysis of layered wooden shells using an orthotropic elasto-plastic model for multi-axial loading of clear spruce wood. *Journal of Computational and Applied Mathematics, 194*, 2661–2685. doi:10.1016/j.cma.2004.07.051.
Moore, J. R., & Maguire, D. A. (2008). Simulating the dynamic behavior of Douglas-fir trees under applied loads by the finite element method. *Tree Physiology, 28*, 75–83. doi:10.1093/treephys/28.1.75.
Ormarsson, S., Dahlblom, O., & Johansson, M. (2010). Numerical study of how creep and progressive stiffening affect the growth stress formation in trees. *Trees-Structure and Function, 24*, 105–115. doi:10.1007/s00468-009-0383-3.
Ozyhar, T., Hering, S., & Niemz, P. (2013). Moisture-dependent orthotropic tension-compression asymmetry of wood. *Holzforschung, 67*, 395–404.
Ross, R. J. (2010). In R. J. Ross (Ed.), *Wood Handbook: wood as an engineering material*. Madison Wisconsin: Forest Products Laboratory.
Salençon, J. (2001). *Handbook of continuum mechanics: general concepts, thermoelasticity*. Berlin; New York: Springer.
Sellier, D., Fourcaud, T., & Lac, P. (2006). A finite element model for investigating effects of aerial architecture on tree oscillations. *Tree Physiology, 26*, 799–806. doi:10.1093/treephys/26.6.799.
Skaar, C. (1988). Wood-Water Relations. Springer-Verlag Berlin Heidelberg.
Tsai, S. W., & Wu, E. M. (1971). General theory of strength for anisotropic materials. *Journal of Composite Materials, 5*, 58–80.
Wagner, L., Bader, T. K., Auty, D., & de Borst, K. (2012). Key parameters controlling stiffness variability within trees: a multiscale experimental–numerical approach. *Trees-Structure and Function, 27*, 321–336. doi:10.1007/s00468-012-0801-9.
Walker, J. (1961). *Interpretation and measurement of strains in wood. (PhD Thesis)*. West Lafayette, IN, USA: Purdue University Engineering Department.
Zobel, B. J., & Sprague, J. R. (1998). *Juvenile wood in forest trees*. Berlin, Heidelberg: Springer, Berlin Heidelberg.

Submit your manuscript to a SpringerOpen journal and benefit from:

► Convenient online submission
► Rigorous peer review
► Immediate publication on acceptance
► Open access: articles freely available online
► High visibility within the field
► Retaining the copyright to your article

Submit your next manuscript at ► springeropen.com